THE ASTROPHYSICAL JOURNAL, 561:L157–L160, 2001 November 10

CHANDRA DETECTION OF THE RADIO AND OPTICAL DOUBLE HOT SPOT OF 3C 351

G. BRUNETTI,[1,2] M. BONDI,[1] A. COMASTRI,[3] M. PEDANI,[4]
S. VARANO,[2] G. SETTI,[1,2] AND M. J. HARDCASTLE[5]
Received 2001 September 4; accepted 2001 October 3; published 2001 October 19

ABSTRACT

In this Letter, we report a *Chandra* X-ray detection of the double northern hot spot of the radio quasar 3C 351. The hot spot has also been observed in the optical with the *Hubble Space Telescope* (*R* band) and with the 3.5 m Telescopio Nazionale Galileo (*B* band). The radio-to-optical and X-ray spectra are interpreted as the results of the synchrotron and synchrotron self-Compton mechanisms, respectively, with hot spot magnetic field strengths ~3 times smaller than the equipartition values. In the framework of shock acceleration theory, we show that the requirement for such a relatively small field strength is in agreement with the fitted synchrotron spectral models and with the sizes of the hot spots. Finally, we show that the combination of a lower magnetic field strength with the high frequencies of the synchrotron cutoff in the fitted synchrotron spectra provides strong evidence for electron acceleration in the hot spots.

Subject headings: acceleration of particles — quasars: individual (3C 351) — radiation mechanisms: nonthermal

1. INTRODUCTION

It is generally assumed that the relativistic particles in powerful radio galaxies and quasars, initially generated in the vicinity of the active galactic nucleus and channeled by the radio jets out to hundreds of kiloparsecs, are reaccelerated in the radio hot spots, which mark the location of strong planar shocks formed at the heads of the jets themselves (e.g., Begelman, Blandford, & Rees 1984; Meisenheimer et al. 1989). One of the most important pieces of evidence in favor of electron reacceleration in the hot spots is the detection of synchrotron emission in the optical/near-IR band, due to high-energy electrons (Lorentz factor $\gamma > 10^5$) with very short radiative lifetimes (e.g., Meisenheimer, Yates, & Röser 1997 and references therein). X-ray observations of nonthermal emission from the radio hot spots are of fundamental importance to constrain the energetics and the spectrum of the relativistic electrons and to test the reacceleration scenario. Until the advent of *Chandra*, nonthermal X-ray emission had been detected from only a few hot spots. One well-known detection was the *ROSAT* Position Sensitive Proportional Counter observation of the radio hot spots of Cygnus A (Harris, Carilli, & Perley 1994), where the hot spot emission was interpreted as synchrotron self-Compton (SSC) emission, implying magnetic field strengths in the hot spots close to the equipartition values. *Chandra* has enabled significant progress in this field, with a number of successful detections in the first 2 years of observations (3C 295: Harris et al. 2000; Cyg A: Wilson, Young, & Shopbell 2000; Pictor A: Wilson, Young, & Shopbell 2001; 3C 123: Hardcastle, Birkinshaw, & Worrall 2001; 3C 207: Brunetti et al. 2001; 3C 263: M. J. Hardcastle et al. 2001, in preparation). With the exception of Pictor A, the best and most straightforward interpretation for the X-ray emission in these objects is provided by the SSC mechanism under approximate equipartition conditions.

In this Letter, we report on the *Chandra* discovery of X-ray emission from the double northern hot spot of 3C 351 (components J and L of Bridle et al. 1994) and on the modeling of the broadband spectrum. The values $H_0 = 50$ km s^{-1} Mpc^{-1} and $q_0 = 0.5$ are assumed throughout; 1″ corresponds to 6.2 kpc at the redshift of 3C 351. Reported errors are at the 90% confidence level.

2. TARGET AND DATA ANALYSIS

The powerful double-lobed radio source 3C 351 is identified with a quasar at a redshift $z = 0.371$ (Laing, Riley, & Longair 1983). In addition to the *Chandra* data, we have analyzed Very Large Array (VLA) and *Hubble Space Telescope* (*HST*) archive data and obtained new *B*-band observations with the 3.5 m Telescopio Nazionale Galileo (TNG).

2.1. *Radio and Optical Data*

Table 1 lists the observations used in this Letter and the derived flux densities at different frequencies. The 1.4 GHz values are derived from an A + B configuration VLA image published by Leahy & Perley (1991). Excellent high-resolution deep radio images at 5 GHz have been published by Bridle et al. (1994), and the 5 GHz flux density of 3C 351J is from this paper. Higher frequency radio fluxes have been obtained by reducing archive VLA observations at 15 and 22 GHz. Standard procedures for calibration and deconvolution were applied to the data. The fluxes of the hot spots were corrected for primary beam attenuation and for atmospheric opacity.

Röser (1989) first discovered the northern radio hot spots in the optical band, whereas Lähteenmäki & Valtaoja (1999) found optical linear polarization (*I* and *V* bands) with the 2.5 m Nordic Optical Telescope on La Palma; to our knowledge, no optical fluxes have been quoted in the literature. On 1995 November 29, 3C 351 was observed with the Wide Field Planetary Camera 2 (WFPC2) on the *HST* for 2400 s using the filter F702W (close to the *R* band). We analyzed these *HST* observations in the standard manner, removing cosmic rays and

[1] Istituto di Radioastronomia del CNR, via Gobetti 101, I-40129 Bologna, Italy.
[2] Dipartimento di Astronomia, Università di Bologna, via Ranzani 1, I-40127 Bologna, Italy.
[3] Osservatorio Astronomico di Bologna, via Ranzani 1, I-40127 Bologna, Italy.
[4] Centro Galileo Galilei, Santa Cruz de La Palma, Canary Islands E-38700, Spain.
[5] Department of Physics, University of Bristol, Tyndall Avenue, Bristol BS8 1TL, UK.

TABLE 1
OBSERVATIONS

Band	Frequency	Telescope	Flux J (mJy)	Flux L (mJy)
Radio	1.4 GHz	VLA A + B	480[a]	1290[a]
	4.9 GHz	VLA A + B	201[b]	...
	15.0 GHz	VLA C	85	219
	22.0 GHz	VLA C	72	174
Optical	*R*	*HST*	2.5E−3	3.8E−3
	B	TNG	1.5E−3	1.3E−3
X-ray	1 keV	*Chandra*	(5.2 ± 1.1)E−6	(3.4 ± 1.1)E−6

NOTE.—Errors on radio fluxes (1.4–15 GHz) are within 5%, whereas those on 22 GHz and optical fluxes are within 10%.
[a] From Leahy & Perley 1991.
[b] From Bridle et al. 1994.

using the bright quasar nucleus to correct the astrometry. On the basis of positional coincidence, we identified optical counterparts of the two northern radio hot spots on the WFPC2 image. In order to better constrain the optical spectra, we also observed these hot spots with a 1200 s *B*-band exposure at the 3.5 m TNG on La Palma during the night of 2001 August 16. The hot spots were detected with a high signal-to-noise ratio, and the errors on the fluxes (Table 1), obtained with 4″ aperture photometry (the seeing was 1.″5), are within 10%.

2.2. *X-Ray Data*

We have analyzed archival data on 3C 351 observed for 9.8 ks with the *Chandra* observatory on 2000 June 1 in a guaranteed time observation. The raw level 1 data were reprocessed using the latest version (CIAO2.1) of the CXCDS software. We generated a clean data set by selecting the standard grades (0, 2, 3, 4, 6) and energies in the band 0.1–10 keV. The X-ray image is shown in Figure 1, with superposed contours of the 1.4 GHz VLA radio image. In addition to the nuclear source, two relatively bright X-ray sources, coincident with the double northern radio hot spot, are clearly detected: ~82 ± 10 and 54 ± 9 net counts are associated with components J and L, respectively. Despite the poor statistics, we have attempted to derive spectral information using appropriate response and effective area functions. In both cases, a single power law (3C 351J: $\alpha = 1.2 \pm 0.5$; 3C 351L: $\alpha = 1.7 \pm 1.2$), with absorption fixed at the Galactic value $N_{\rm H} = 2.26 \times 10^{20}$ cm^{-2} (Elvis, Lockman, & Wilkes 1989), provides an acceptable description of the data.

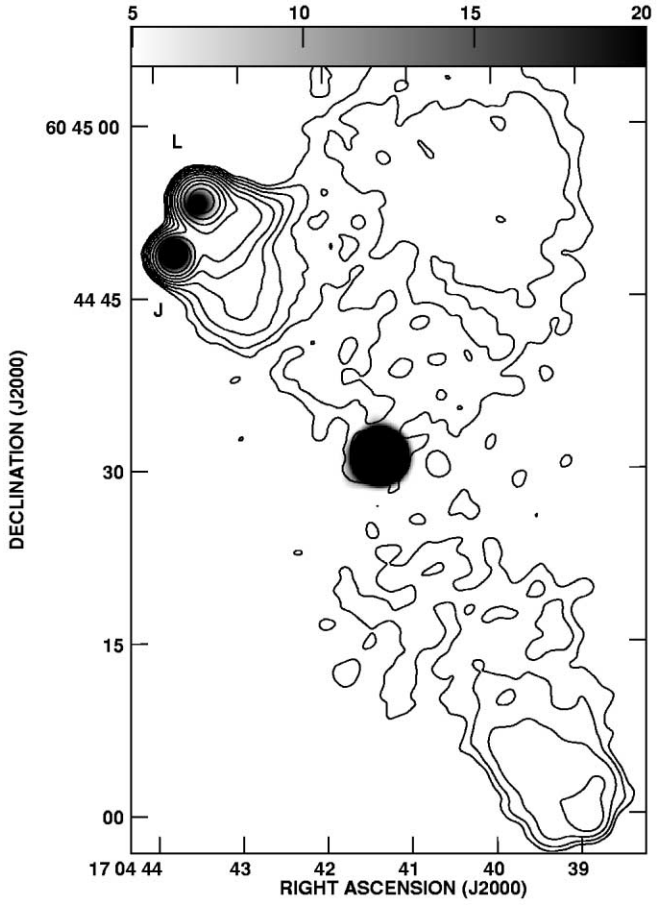

FIG. 1.—The 1.4 GHz VLA data (*contours*) overlaid on the 0.3–8 keV Advanced CCD Imaging Spectrometer *Chandra* image (*gray scale*). The radio contours are 1.0 × (−1, 1, 2, 4, ...) mJy beam^{-1}; beam = 1.″85.

3. EMISSION PROCESSES AND ELECTRON ACCELERATION

3.1. *Modeling the Broadband Spectrum*

As no bright thermal emission from a cluster around 3C 351 has been detected by the *Chandra* observation, we find that X-ray emission from any shocked gas in the hot spot region would be orders of magnitude lower than that observed. As discussed in § 1, the most plausible nonthermal mechanism responsible for X-ray emission is SSC. In Figure 2, we show fits to the broadband spectrum of the hot spots 3C 351J and L. The emitted synchrotron and SSC spectra are obtained with standard recipes, assuming an electron energy distribution as derived under basic Fermi-I acceleration theory: a power-law spectrum with injection energy index δ steepens at higher energies ($\gamma > \gamma_b$) up to a high-energy cutoff γ_c, whereas it flattens at lower energies before a low-energy cutoff (equations for the electron spectrum and for the SSC calculation are given in Brunetti et al. 2001, eqs. [2]–[9] and Appendix A). The SSC flux is obtained by taking radii $R_{\rm J} = 0.''1$ and $R_{\rm L} = 0.''5$ for 3C 351J and L, respectively (Bridle et al. 1994). The parameters of the spectra obtained from fitting the radio and optical data points, i.e., the electron injection index (δ), the synchrotron break (ν_b), and cutoff frequency (ν_c) are given in Table 2 (90% confidence level). A synchrotron spectrum with a cutoff frequency at very high energies is still consistent with the data of 3C 351J and is also plotted in Figure 2 in order to show the maximum synchrotron contribution to the X-rays (≤30% at 90% confidence level). It should be noted that the high-frequency cutoff of 3C 351J is at least 1 order of magnitude larger than those of other optical hot spots in the literature and that the break frequencies for both hot spots are also higher than the typical breaks measured in the synchrotron spectra of

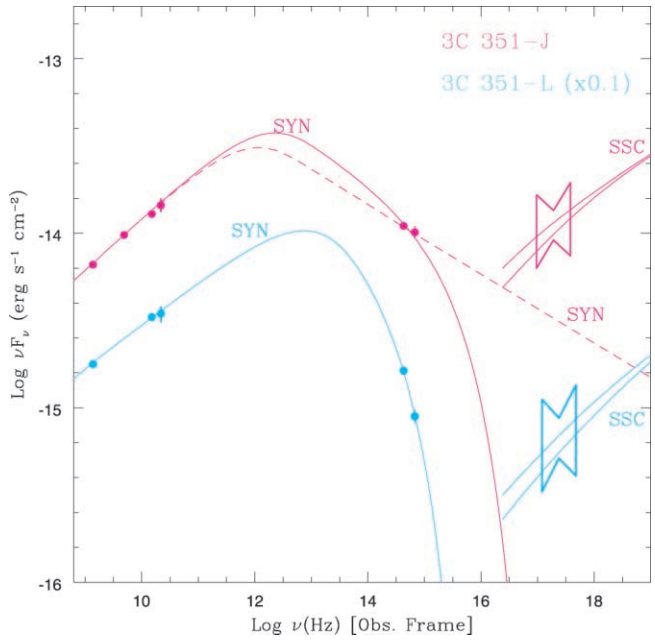

FIG. 2.—Synchrotron and SSC models (*solid lines*) compared with the data of 3C 351J (*magenta*) and L (*cyan*). For 3C 351J, the synchrotron model (*solid line*) has $\delta = 2.4$, $\nu_b = 3.2 \times 10^{12}$ Hz, and $\nu_c = 1.2 \times 10^{16}$ Hz. The corresponding SSC models are calculated with $B = 70$ μG and with a low-frequency cutoff in the synchrotron photons at 100 MHz (*lower curve*) and 1 MHz (*upper curve*). A synchrotron model with $\nu_b = 1.6 \times 10^{12}$ Hz and no cutoff is also shown (*dashed line*). For 3C 351L, the synchrotron model has $\delta = 2.5$, $\nu_b = 2.2 \times 10^{13}$ Hz, and $\nu_c = 1.1 \times 10^{15}$ Hz. The corresponding SSC models are calculated with $B = 35$ μG, with the other parameters as in the case of 3C 351J. The fluxes of 3C 351L are reported in the panel multiplied by a factor of 0.1.

optical hot spots (e.g., Meisenheimer et al. 1997; Gopal-Krishna et al. 2001).

We find that for both hot spots the SSC mechanism provides a good representation of the *Chandra* data for magnetic fields, ($B_{\rm IC}$, Table 2), which are a factor of ~3 smaller than the equipartition values ($B_{\rm eq} \simeq 230$ μG for 3C 351J and $B_{\rm eq} \simeq 100$ μG for 3C 351L). For these field strengths, we find that inverse-Compton (IC) scattering of cosmic microwave background (CMB) photons could account for ~10% of the X-ray flux of 3C 351L, whereas it does not significantly contribute to the X-ray spectrum of 3C 351J. It is interesting to note that the X-ray luminosity of 3C 351J is comparable to or slightly higher than the synchrotron radio-to-optical luminosity. If the X-rays are of SSC origin, the radiative losses of the relativistic electrons would be dominated by IC (due to second- and third-order scattering) so that the electrons' cooling times would be a factor of ~4 shorter than those due to the synchrotron process alone. However, as the value of the magnetic field strength in the Compton-dominated 3C 351J is ~3 times smaller than equipartition, the radiative cooling time of the electrons emitting synchrotron radiation at $\sim 10^{16}$ Hz is a factor of ~2.5 larger than that computed under equipartition, so that the acceleration of such particles is eased with respect to the equipartition case. A viable model for the X-ray emission of 3C 351J can also be obtained with a combination of a synchrotron spectrum and an SSC component (accounting for ≥70% of the flux). In this case, the resulting spectral index would be somewhat steeper than that of the SSC model. This would imply very efficient electron acceleration processes, but the basic SSC model remains unchanged. Improved spectral measurements may be able to settle the size of a possible synchrotron contribution.

TABLE 2

SPECTRAL PARAMETERS AND *B*-FIELDS

Hot Spot	δ	ν_b ($\times 10^{13}$ Hz)	ν_c ($\times 10^{14}$ Hz)	$B_{\rm IC}$ (μG)
L	2.5	3.6 ± 3.0	11 ± 7	35
J	2.4	0.35 ± 0.25	≥90	70

Relativistic boosting appears to be necessary to explain the X-ray jet emission in a few core-dominated radio-loud quasars (e.g., Tavecchio et al. 2000; Celotti, Ghisellini, & Chiaberge 2001; Brunetti et al. 2001). However, its role in the case of the hot spots is still unclear; for instance, statistical analysis of samples of FR II radio sources implies nonrelativistic velocities (e.g., Arshakian & Longair 2000). Under equipartition (in the hot spot frame), IC scattering of CMB photons can produce the observed X-ray fluxes for Doppler factors $\mathcal{D} \sim 8$ and 3.8 in the cases of 3C 351J and L, respectively. Such factors, however, can be obtained only for relatively small angles between the hot spots' velocities and the line of sight ($\theta \leq 6°$ with $\Gamma_{\rm bulk} > 4$ for 3C 351J and $\theta \leq 15°$ with $\Gamma_{\rm bulk} > 2$ for 3C 351L), whereas the radio properties of 3C 351 and the lack of lobe asymmetry suggest much larger inclination angles and smaller hot spot velocities. This problem remains even if we relax the equipartition condition: assuming a departure from equipartition similar to that required by the SSC, a Doppler factor $\mathcal{D} \sim 4.5$ ($\theta \leq 10°$) is necessary to match the X-ray flux of 3C 351J by IC scattering of the CMB. A second possible way of accounting for the large X-ray fluxes of the hot spots is to require the SSC to be enhanced with respect to the synchrotron emission via Doppler deboosting. We find, however, that in order to match the data under equipartition conditions, $\mathcal{D} \sim 0.25$ is required, implying extremely high bulk Lorentz factors ($\Gamma_{\rm bulk} \sim 15$–$30$, with $\theta \sim 30°$–$40°$).

3.2. *Is In Situ Reacceleration Necessary?*

Based on evidence for relativistic jet bulk motion out to 100 kpc scales, Gopal-Krishna et al. (2001) have reconsidered a minimum loss scenario in which the relativistic electrons, accelerated in the central active nucleus, flow along the jets losing energy only because of the inescapable IC scattering of CMB photons. Under these assumptions, comparing the electron radiative lifetime with the travel time to the hot spots, they find that in situ electron reacceleration is, in general, not absolutely necessary to explain the optical/near-IR synchrotron radiation from the hot spots so far detected. Following Gopal-Krishna et al. (2001), we define $\eta = D_{\rm obs}/D_{\rm max}$, the ratio between the distance of the hot spots from the nucleus and the largest distance covered by the electrons in the jet before dropping to less than e^{-1} of their initial energy due to IC losses; i.e.,

$$D_{\rm max}({\rm kpc}) \simeq 145 \frac{\beta_{\rm bulk} \sin\theta}{\Gamma_{\rm bulk}(1+z)^{4.5}} \left[\frac{B(\mu{\rm G})}{\nu_c(10^{14}\ {\rm Hz})}\right]^{1/2}. \quad (1)$$

With $\theta \sim 30°$ and our constraints on ν_c and B, we find $\eta \geq$ 26–110 (3C 351J) and $\eta \sim$ 9–38 (3C 351L) for $\Gamma_{\rm bulk} = 2$–10 (as adopted by Gopal-Krishna et al. 2000). We also find that if the electrons are accelerated in 3C 351J and then transported in a jet out to 3C 351L, the lifetime of the optically emitting electrons in 3C 351L ($\sim 5 \times 10^4$ yr assuming $B \geq 10$ μG in the jet) is at least 1 order of magnitude less than the time necessary to cover the distance between the two hot spots at

nonrelativistic speeds, and η is still greater than 2.2 if they are transported at relativistic speeds. These large values unequivocally point to the necessity of efficient reacceleration processes in both northern hot spots of 3C 351.

3.3. *Electron Acceleration in the Hot Spot*

An independent estimate of the magnetic field strength B in the hot spot can be obtained in the framework of shock acceleration models. The highest energies of the relativistic electrons accelerated in a shock region by Fermi processes is given by the ratio between gain and loss terms. For a strong shock (here, for simplicity, we consider the nonrelativistic case), the largest energy of the accelerated electrons is (e.g., Meisenheimer et al. 1989)

$$\gamma_c \propto u_-^2 B_+^{-2} \lambda_+(B_+)^{-1}, \quad (2)$$

where u_- is the velocity of the flow in the upstream region (with respect to the shock), $B_+ = (B_{\rm IC}^2 + B^2)^{1/2}$ is the total equivalent magnetic field strength in the downstream region, and $\lambda_+(B_+)$ is the mean free path of the relativistic electrons in the downstream region.

The break energy of the electrons in the downstream region (i.e., the highest energy of the oldest electrons in the postshock region) is

$$\gamma_b = \frac{\gamma_c}{1 + C\,(l/u_+)\,B_+^2 \gamma_c} \propto \frac{u_+}{l} B_+^{-2}, \quad (3)$$

where u_+ is the velocity of the flow in the downstream region, l is the linear extension of such a region, and C is a constant. Substituting into equations (2) and (3) the expression for the synchrotron cutoff frequency, $\nu_c \propto \gamma_c^2 B$, one obtains

$$B_+ \sim 2.3 \left[\frac{u_+}{0.3}\left(\frac{\gamma_c}{\gamma_b} - 1\right)\right]^{2/3} l_{\rm kpc}^{-2/3} \left(\frac{\nu_c}{10^{15}\ {\rm Hz}}\right)^{-1/3} \xi^{1/3}, \quad (4)$$

where $\xi = B/B_+$ is $\simeq$0.5 for hot spot J and 0.9 for L, and the value of $l_{\rm kpc}$ can be estimated from Bridle et al. (1994). For $\gamma_c/\gamma_b \gg 1$, equation (4) reduces to $B_+ \propto \nu_b^{-1/3}$, and from the values of ν_b previously constrained we find $B \sim 80$ and 30 μG for J and L, respectively, with a formal uncertainty of about a factor of 2. These values are in good agreement with the magnetic field strengths implied by an SSC origin for the X-ray emission.

4. CONCLUSIONS

The radio-to-optical spectrum of the two northern hot spots of 3C 351 is well accounted for by a synchrotron model under the standard shock acceleration scenario. The most straightforward interpretation of the X-ray emission discovered by *Chandra* is the SSC mechanism. A viable model for 3C 351J is also given by a combination of SSC and synchrotron spectra, with the SSC accounting for $\geq$70% of the X-ray flux. In order to match the X-ray fluxes, a magnetic field strength of a factor of 3 lower than the equipartition value is required in both the hot spots. In principle, the assumption of relativistic bulk motion of the hot spots might reduce the departure from equipartition, but large ad hoc distortions of the radio jet would be required, with the hot spots moving closer to the line of sight. The frequencies of the cutoff in the synchrotron spectra and the magnetic field strengths point to the need for in situ electron (re)acceleration in the region of both the hot spots. When we independently estimate the magnetic field strength of the hot spots, using relationships from standard shock theory, our results are consistent with the more precise value obtained by modeling the X-ray emission as resulting from the SSC mechanism.

This work is partially supported by the Italian Ministry for University and Research (MURST) under grants Cofin99-02-37 and Cofin00-02-36. This Letter is based on observations made with the Italian TNG, operated on the island of La Palma by the Centro Galileo Galilei of the CNAA at the Spanish Observatorio del Roque de los Muchachos of the Instituto de Astrofisica de Canarias. We would like to thank R. Fanti for very useful discussions and A. Zacchei for technical support.

REFERENCES

Arshakian, T. G., & Longair, M. S. 2000, MNRAS, 311, 846
Begelman, M. C., Blandford, R., & Rees, M. J. 1984, Rev. Mod. Phys., 56, 255
Bridle, A. H., Hough, D. H., Lonsdale, C. J., Burns, J. O., & Laing, R. A. 1994, AJ, 108, 766
Brunetti, G., Bondi, M., Comastri, A., & Setti, G. 2001, A&A, in press
Celotti, A., Ghisellini, G., & Chiaberge, M. 2001, MNRAS, 321, L1
Elvis, M., Lockman, F. J., & Wilkes, B. J. 1989, AJ, 97, 777
Gopal-Krishna, Subramanian, P., Wiita, P. J., & Becker, P. A. 2001, A&A, 377, 827
Hardcastle, M. J., Birkinshaw, M., & Worrall, D. M. 2001, MNRAS, 323, L17
Harris, D. E., Carilli, C. L., & Perley, R. A. 1994, Nature, 367, 713
Harris, D. E., et al. 2000, ApJ, 530, L81
Lähteenmäki, A., & Valtaoja, E. 1999, AJ, 117, 1168
Laing, R. A., Riley, J. M., & Longair, M. S. 1983, MNRAS, 204, 151
Leahy, J. P., & Perley, R. A. 1991, AJ, 102, 537
Meisenheimer, K., et al. 1989, A&A, 219, 63
Meisenheimer, K., Yates, M. G., & Röser, H.-J. 1997, A&A, 325, 57
Röser, H.-J. 1989, in Lect. Notes Phys. 327, Hot Spots in Extragalactic Radio Sources, ed. K. Meisenheimer & H.-J. Röser (Berlin: Springer), 91
Tavecchio, F., Maraschi, L., Sambruna, R. M., & Urry, C. M. 2000, ApJ, 544, L23
Wilson, A. S., Young, A. J., & Shopbell, P. L. 2000, ApJ, 544, L27
———. 2001, ApJ, 547, 740